

Luminescence Methods

Sample Preparation

Luminescence samples were processed under a dimmed 589-nm sodium lamp fitted with a Lee 101 filter. Following overnight treatments in 10% HCl and H₂O₂, the 150–250 µm size fraction of each luminescence sample underwent multiple density separations in solutions of lithium heteropolytungstate to obtain a quartz fraction ($\rho = 2.57 - 2.70$ g/ml) and a potassium-rich feldspar fraction ($\rho < 2.57$ g/ml). Quartz samples then underwent a 40-min etch in concentrated HF in a ultrasonic bath before a final rinse in 30% HCl, whereas K-feldspar-rich samples were etched for 40 minutes in 10% HF followed by an HCl rinse. All samples were resieved through a 85-µm nylon mesh following HF etching to ensure measurement of large intact grains, although the nominal grain sized used in dose rate calculations remains 150–250 µm.

Instrument, Calibration, and Age Calculations

Sample analyses were performed at Middlebury College on a Daybreak 2200 luminescence reader. All samples (including single grains of feldspar) were analyzed on 9.8-mm diameter aluminum discs with a thickness of 0.5 mm. Photons were recorded using a 9235QA photomultiplier tube manufactured by Electron Tubes with a dark count rate of roughly 20 cps. Stimulation was performed with blue LEDs (480 nm) for quartz and infrared LEDs (880 nm) for feldspar. For quartz analyses, measured light was filtered using a Schott UG-11 and Edmunds UG-340 filter pack with an approximate admittance window from 260 to 390 nm, peaked at ~330 nm. Feldspar analyses were filtered with an Edmunds BG-39 and Kopp 759 filter pack with an admittance window of 320 to 480 nm that peaked at ~380 nm.

Irradiations were performed using a nominal 100 mCi ⁹⁰Sr beta source. Source calibration was previously performed with two different sets of gamma-irradiated calibration quartz: Riso batches 71 and 98. Because batch 71 is not thermally annealed and batch 98 is these two calibration standards give very different sensitivity changes during the SAR protocol. Nonetheless, accepting only analyses for which the first and second test dose response of a given aliquot agree to within 5% yields tight agreement between the two standards and a nominal dose rate of 0.0505 ± 0.0025 Gy/s (2-sigma uncertainty) as of June 4th, 2019.

All samples in this study were analyzed using the SAR protocol for quartz [1] and the post-infrared infrared SAR (pIRIR SAR) protocol for K-feldspar [2]. Both protocols involved six SAR cycles, for example: natural, regen-1, regen-2, regen-3, zero dose, and regen-1'. To improve efficiency, analyses were run in a multi-step process. First, a 'recon' stage involved measuring the first two cycles (e.g. Natural, TD_N, Regen-1, and TD₁) to assess brightness and test dose reproducibility. A net signal of > 40 cps and TD_N/TD₁ ratio between 0.9 and 1.1 was required for a disc to continue to the 'finish' stage. Typically 15–50% of grains were then included in a second 'finish' stage which involved completing the four remaining regenerative cycles and applying rejection criteria as usual.

Small aliquots of quartz (20–50 grains) were shined down with blue LED for 30 seconds at 125 °C, following a cut heat temperature of 160 °C or a preheat temperature of 225 °C (Figure S1). Due to the very dim nature of the quartz, we were unable to perform a preheat plateau test. However, dose recovery tests on selected bright aliquots of quartz revealed recovery of the administered dose to within 5%. Single grains of K-feldspar were shined down twice for 80 seconds with an IR LED, following a preheat of 250 °C (Figure S1). The first shine down was performed at 50 °C, followed by a high temperature shine down at 225 °C. For feldspar, an 80-second bleach at 235 °C was performed after each of the six measurement cycles. A temperature of 225 °C was chosen for the second shine down because it represents a compromise between the increased fading observed at lower temperatures and the increased residual doses observed at higher temperatures [2].

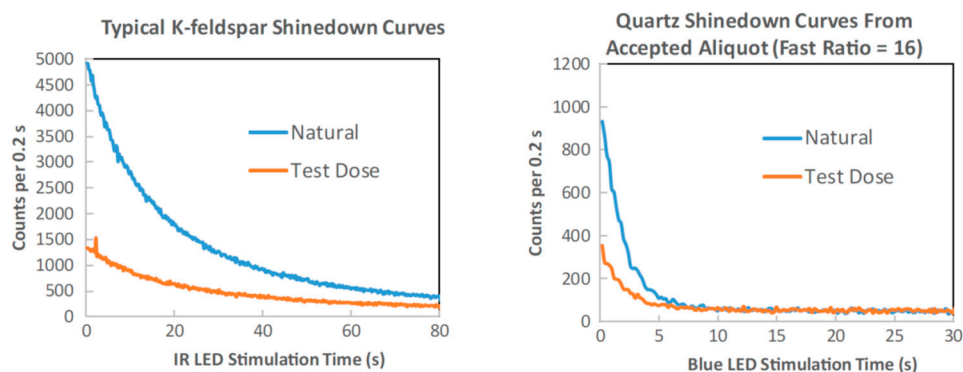


Figure S1. Example shine down curves for quartz (blue LED) and K-feldspar (IR LED).

Data reduction was conducted using an Excel spreadsheet originally authored by Ronald Goble and subsequently modified by Tammy Rittenour, Sebastien Huot, and Zach Perzan. Because most accepted quartz aliquots in this study have fast ratios between 10 and 20, net signals were computed using early background correction by subtracting the mean counts in the fourth–sixth seconds from the mean counts within the first 0.6 seconds. Net signals for feldspar were computed by subtracting the mean signal in the 10th to 15th seconds from the mean signal in the first two seconds of the shine down. Equivalent dose (D_e) and associated uncertainties were estimated by fitting a quadratic function to all of the regenerative data points, including the measured zero dose. An additional uncertainty was propagated to reflect intrinsic variability in measured dose rate distributions beyond those already accounted for by curve-fitting [3]. This was 5% for small aliquots of quartz and 15% for single feldspar grains based on previous in-house experiments to estimate over-dispersion in well-bleached examples of these two sample types.

Four quality criteria were used to reject D_e estimates: the recycling test, recuperation test, and the test-dose reproducibility ratio (the % difference between the first and second test dose), and the fast ratio (quartz only). The cutoff for recycling and test dose reproducibility was 15%, whereas a 10% threshold was used for recuperation, and a fast ratio above 10 was required for quartz aliquots. For quartz, the mean absolute deviations from unity were: 0.07 ± 0.05 % for the recycling ratio, 0.07 ± 0.04 % for the TD_N/TD_1 ratio. The mean recuperation for quartz was 3 ± 2 % and the mean fast ratio was 24 ± 38 . For feldspar, the mean absolute deviations from unity were: 0.04 ± 0.03 % for the recycling ratio, 0.07 ± 0.04 % for the TD_N/TD_1 ratio. The mean recuperation for feldspar was 5.9 ± 3 %.

For quartz samples, an additional “IR check” was administered to verify the purity after the SAR protocol was complete. This was done by applying an additional test dose to the aliquot, preheating it, and then measuring the response to infrared stimulation at room temperature. Quartz samples were characterized by slow dim signals and poor behavior resulting in an acceptance rate of only ~2% for quartz discs. Low net signals and fast ratios were the primary reason for quartz aliquot rejection.

Dose rates were calculated using High Resolution Gamma Spectrometry (HRGS) of sediment collected within a 25-cm radius of each sample tube during excavation [4]. Analyses were performed at Dartmouth College, including measurements of: ^{234}Th , ^{228}Ac , ^{226}Ra , ^{224}Ra , ^{222}Rn , ^{214}Pb , ^{214}Bi , ^{212}Pb , ^{210}Pb , and ^{40}K . Nuclides that were not measured were extrapolated from the closest neighboring isotopes in the decay chain. Nuclide activities were converted to dry alpha, beta, and gamma dose rates using standard conversion factors [4]. Environmental dose rates experienced during burial were then computed in DRAC 1.2 [5] using conversion factors [4], beta grain size attenuation factors [6], and beta etch factors [7].

Direct alpha dose was assumed to be zero given that grains were etched in HF prior to analysis. K content of representative feldspar grains was determined at Middlebury College by EDS analysis on a polished grain mount using a Tescan Vega3 SEM calibrated with a cobalt standard. Internal dose rates for K-feldspar were then calculated using DRAC 1.2 based on an average potassium content of 10.7 ± 1.4 % ($n = 18$). Water contents were computed on sediment collected from a 25-cm radius

around each sample using a mass difference calculation after drying in an oven for two days at 65 °C (wet weight–dry weight at room temperature).

Anomalous Fading and Residual Dose in K-Feldspar

Infrared stimulated luminescence (IRSL) dating of feldspar has been shown to systematically underestimate the known age of some samples due to anomalous fading of the luminescence signal over time [8]. Although the pIRIR approach exploits traps that show less fading than conventional IRSL [2], in some cases this signal still displays nontrivial fading. Recognizing this, a subset of previously analyzed and accepted feldspar grains ($n = 157$) underwent fading tests. Grains analyzed for fading were irradiated with 15 Gy, immediately preheated, and then stored in a dark cabinet for a single storage period ranging from two to eight weeks. They were then analyzed using a full SAR protocol to determine the equivalent dose for each aliquot. A fading parameter or ‘ κ -value’ was then computed following [8] by assuming zero fading at time zero. The resultant κ -values were consistent between samples and yielded an approximately Gaussian distribution with a mean of 0.014 ± 0.007 , which was applied to correct all K-feldspar ages following standard procedures [8] (Figure S2).

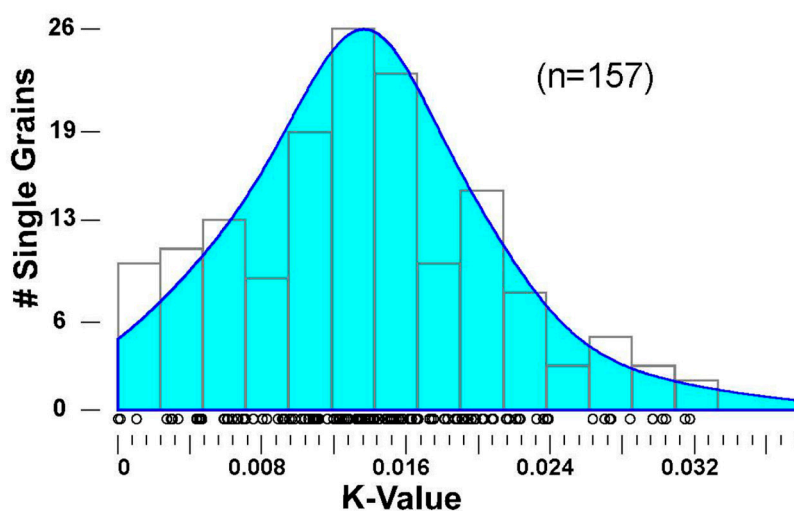


Figure S2. Distribution of κ values measured in 157 K-feldspar grains.

Although the pIRIR₂₂₅ SAR approach reduces anomalous fading, it tends to result in higher residual doses. Residual dose is the component of the signal that is not bleachable by natural light but is released by IR illumination during analysis. Accordingly, the residual dose was measured by mounting fresh K-feldspar grains and exposing them to a full spectrum lightbulb for 96 hours followed by three days in a rooftop greenhouse. These grains were then measured using the identical pIRIR₂₂₅ protocol to regular samples. Unfortunately, residual doses varied over two orders of magnitude from 0.1 to 11 Gy, following a roughly Poisson distribution (Figure S3). A weak relationship was observed between residual dose and the ratio of the first two test doses (TD_N/TD_1), which suggests the residual doses are dependent on the nature of the grain being analyzed (Figure S3). One possibility is that the TD_1/TD_N ratio varies slightly based on the mineralogical properties of the K-feldspar, for example elemental composition of mineral inclusions and that minerals. In this case, grains with a lower TD_1/TD_N ratio might contain electron traps that are less bleachable under natural light. It is also worth considering whether the inverse relationship between the residual dose and TD_1/TD_N could arise due to incorrect normalization of the 225 °C shine down signal as the sensitivity changes between any natural or regenerative shine downs and their subsequent paired test dose. The answer to this question depends on the unknown shift in sensitivity between each paired shine down in a SAR cycle. However, we can explore the ‘worst case’ (and perhaps most likely case) in which there is a much larger drop in sensitivity between the natural shine down and its subsequent paired test dose (TD_N) than there is between subsequent SAR pairs (for example R_1 and

TD₁). In this case, the natural signal is under-corrected relative to the rest of the regenerative curve and the residual dose is underestimated. This scenario would predict an increase in apparent residual dose with increase in TD₁/TD_N, the opposite of what is observed in figure S3, and thus seems a less likely explanation for the observed relationship between TD₁/TD_N and residual dose.

Because the residual dose cannot be measured on the same grains used for De analysis, a linear fit was used to predict a unique residual dose for each feldspar grain as a function of its measured TD_N/TD₁. The relatively large magnitude of estimated residual doses means subtraction of this component is the largest source of error in the K-feldspar ages, as described below.

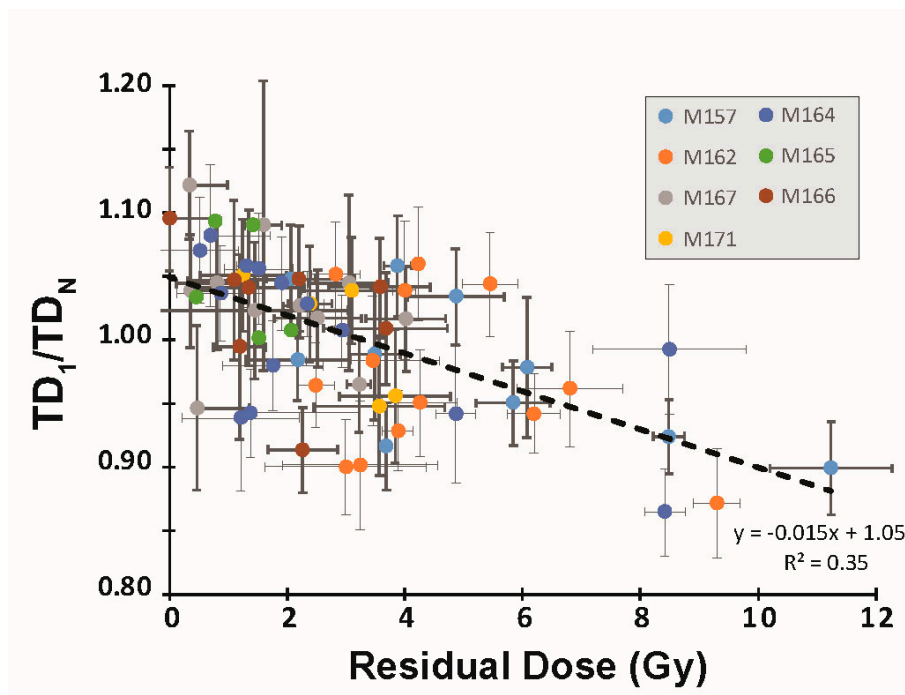


Figure S3. Measured residual doses in K-feldspar grains.

Error Propagation and Age Models

Age estimates were produced using a hybrid data reduction approach in which single aliquot De's were computed using the spreadsheet mentioned above, dose rates were computed using DRAC, and age models were computed using the Rlum software package [9].

Uncertainties on age estimates for single aliquots of quartz were estimated by propagating: (1) the uncertainty on the interpolated De, and (2) a 5% additional analytical uncertainty for small aliquots. Feldspar is more complex, requiring quadratic propagation of: (1) the uncertainty on the interpolated De, (2) a 15% additional analytical uncertainty for single-grain aliquots, (3) uncertainty on the residual dose, and (4) uncertainty on the fading correction. Importantly, the uncertainty introduced by subtraction of the residual dose more than doubles the overall uncertainty, dramatically reducing the apparent overdispersion of the single grain ages (Table S1).

The resultant distribution of ages and uncertainties were then passed to the R-package "Luminescence" for plotting and implementation of age models. All age models were 'logged' meaning that the ages were log-transformed prior to implementing the age models. In this study we opted to use the central age model (CAM) computed from the fully corrected dataset for all samples [10]. The fully corrected CAM ages are roughly 3–4 ka older than the uncorrected age estimates demonstrating the importance of applying a fading correction (Table S1; Figure S4). For feldspar use of the central age model was justified by 0% over-dispersion for all samples. For quartz this was justified by the relatively small number of accepted aliquots, which did not lend confidence in the minimum age model (MAM). Finally, the reported uncertainty on the CAM age estimate was propagated with the dose rate uncertainty provided by the DRAC calculator.

Table S1. Alternate Age Models.

Sample	Aliquots	OD	MAM3	2	IEU	2	CAM	2	OD	MAM3	2	IEU	2	CAM	2	OD	MAM3	2	IEU	2	CAM	2
		<i>full</i>	<i>full</i>		<i>full</i>		<i>full</i>		<i>anal</i>	<i>anal</i>		<i>anal</i>		<i>anal</i>		<i>uncor</i>	<i>uncor</i>		<i>uncor</i>		<i>uncor</i>	
	n_{acc}/n_{tot}	%	ka	ka	ka	ka	ka	ka	%	ka	ka	ka	ka	ka	ka	%	ka	ka	ka	ka	ka	ka
Feldspar PIRIR																						
VT-3-crest	44/300	0	17.6	2.9	10.7	2.1	17.6	1.9	29	5.1	1.3	NC	NC	13.3	1.3	30	4.6	1.1	3.8	0.3	13.8	1.2
TBR5665	47/300	0	15.9	3.2	NC	NC	15.9	1.6	35	4.6	1.1	5.0	0.7	11.9	1.3	37	4.4	0.5	4.9	0.5	12.4	1.3
TBR5648	55/240	0	14.0	2.0	NC	NC	14.0	1.2	16	9.1	1.2	11.1	0.6	11.8	0.7	22	8.0	0.5	9.5	0.5	12.4	0.7
TBR5636	38/120	0	14.3	2.0	NC	NC	14.3	1.4	1	11.6	1.2	NC	NC	11.6	0.6	14	9.3	0.5	11.4	0.5	12.1	0.6
TBR5630	36/240	1	11.6	2.1	NC	NC	11.6	1.5	24	5.3	1.0	5.8	0.8	9.0	0.9	26	4.7	0.5	5.4	0.7	9.4	0.8
TBR5626	32/180	0	11.9	2.5	7.4	1.5	11.9	1.6	32	3.3	1.0	3.5	1.1	8.9	1.1	34	3.0	0.7	3.7	1.4	9.3	1.1
TBR5620	32/120	0	9.5	2.4	6.5	1.2	9.5	1.4	37	3.7	0.8	4.0	0.5	6.8	1.0	40	3.5	0.3	3.8	0.3	7.2	1.0

full: denotes model ages computed with fading and residual corrections and full error propagation

anal: denotes model ages computed on PIRIR SAR results after propagating excess analytical uncertainty but without correcting for fading or residual dose

uncor: denotes model ages computed on PIRIR SAR results without propagating excess analytical uncertainty or correcting for fading or residual dose

NC denotes datasets for which the IEU age model did not converge on a solution

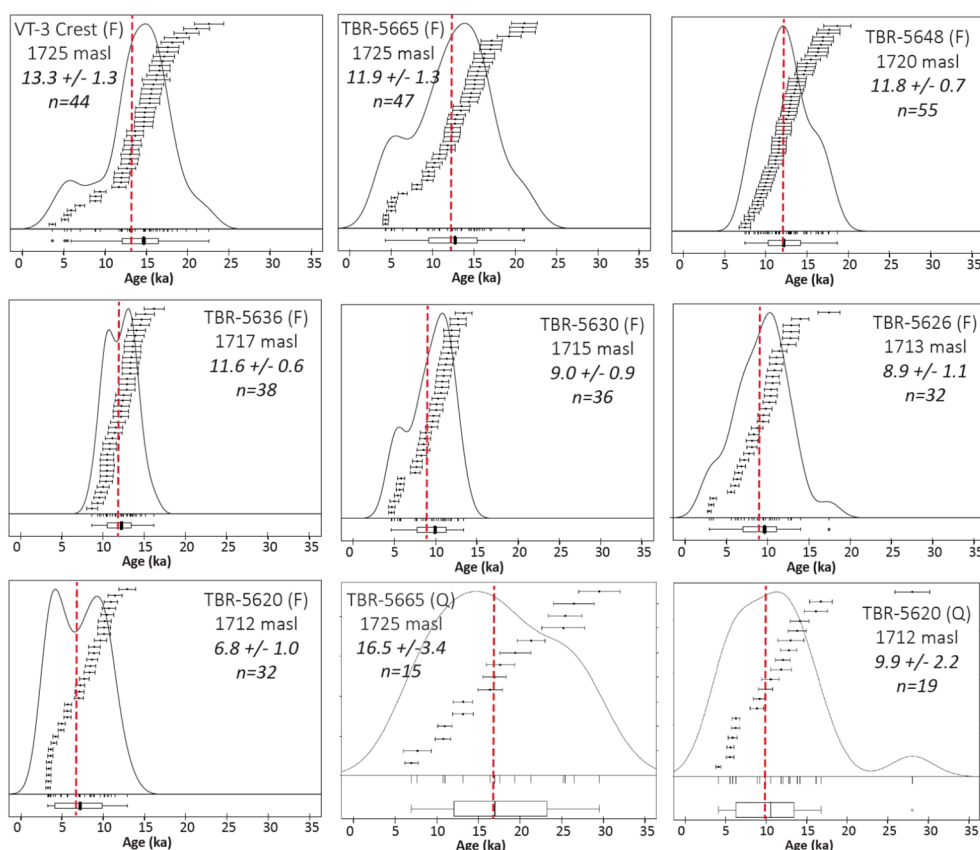


Figure S4. Luminescence results in which K-feldspar grains (F) are plotted without correction for residual dose or fading. An additional analytical uncertainty of 15% has been added to each feldspar analysis. Quartz results (Q) are plotted with a 5% added analytical uncertainty, identical to Figure 11 in the main text.

References Cited in Supplemental Methods

1. Murray, A.S.; Wintle, A.G. Luminescence dating of quartz using an improved single-aliquot regenerative-dose protocol. *Radiat. Measur.* **2000**, *32*, 57–73.
2. Buylaert, J.-P.; Murray, A.S.; Thomsen, K.J.; Jain, M. Testing the potential of an elevated temperature IRSL signal from K-feldspar. *Radiat. Measur.* **2009**, *44*, 560–565.
3. Thomsen, K.J.; Murray, A.; Bøtter-Jensen, L.; Kinahan, J. Determination of burial dose in incompletely bleached fluvial samples using single grains of quartz. *Radiat. Measur.* **2007**, *42*, 370–379.
4. Guérin, G.; Mercier, N.; Adamiec, G. Dose-rate conversion factors: update. *Ancient TL* **2011**, *29*, 5–8.
5. Durcan, J.A.; King, G.E.; Duller, G.A. DRAC: Dose Rate and Age Calculator for trapped charge dating. *Quat. Geochronol.* **2015**, *28*, 54–61.
6. Guérin, G.; Mercier, N.; Nathan, R.; Adamiec, G.; Lefrais, Y. On the use of the infinite matrix assumption and associated concepts: a critical review. *Radiat. Measur.* **2012**, *47*, 778–785.
7. Brennan, B. Beta doses to spherical grains. *Radiat. Measur.* **2003**, *37*, 299–303.
8. Huntley, D.J.; Lamothe, M. Ubiquity of anomalous fading in K-feldspars and the measurement and correction for it in optical dating. *Can. J. Earth Sci.* **2001**, *38*, 1093–1106.
9. Kreutzer, S.; Schmidt, C.; Fuchs, M.C.; Dietze, M.; Fischer, M.; Fuchs, M. Introducing an R package for luminescence dating analysis. *Ancient TL* **2012**, *30*, 1–8.
10. Galbraith, R.F.; Roberts, R.G.; Laslett, G.; Yoshida, H.; Olley, J.M. Optical dating of single and multiple grains of quartz from Jinmium Rock Shelter, northern Australia: Part I, experimental design and statistical models*. *Archaeometry* **1999**, *41*, 339–364.

